JOURNAL OF CATALYSIS 137, 513–522 (1992)

The Morphology of Oxide-Supported MoS_2

MoS_2 supported on oxides such as alumina and promoted with nickel or cobalt constitutes an active catalyst for reactions such as hydrogenation, hydrodesulfurization, and methanation (*1*). Recent work (*2*) has shown that the support oxide has a marked effect on the specific activity of the sulfide catalysts, and it has been suggested that these activity differences may be related to the morphology of the MoS_2 on the surface. MoS_2 is synthesized by sulfiding a supported molybdenum (Mo^{+6}) oxide in 10% H_2S/H_2 at 600–900 K. It is now accepted that on alumina, after a standard calcination at 773 K and independent of the method of preparation (*3*), MoO_3 forms a "monolayer" containing octahedral Mo^{+6} anchored to the surface with Mo–O–Al bonds. A portion of the Mo which is harder to reduce is believed to be incorporated in tetrahedral sites in the alumina (*4*). Evidence for the dispersed molybdena comes from CO_2 chemisorption studies which show a decrease in exposed alumina, and from IR spectroscopy which shows a drop in the surface hydroxyl concentration with the addition of Mo to alumina (*5*). X-ray photoelectron spectroscopic measurements as a function of Mo loading also support this conclusion (*6*). When the concentration of molybdena exceeds that of a monolayer ($\approx$5 Mo/nm^2), three-dimensional crystals of MoO_3 are also observed in addition to the monolayer phase (*6*).

During sulfiding of the MoO_3 in 10% H_2S/H_2 at temperatures in excess of 673 K, the supported molybdenum oxide transforms into MoS_2 and some of the hydroxyls on the alumina surface reappear (*5*). Based on these results, it was originally proposed that microcrystalline MoS_2 sheets are edge-bonded to the surface of the oxide support (*5*). However, Zmierczak *et al.* (*6*) have argued that the crystallization into MoS_2 should directly lead to a partial exposure of the alumina surface, since the specific volume of the MoS_2 is considerably less than that of the dispersed molybdenum (Mo^{+6}) oxide. Their calculations assume that the structure of the MoS_2 is very similar to that of bulk MoS_2, a conclusion supported by EXAFS spectroscopy (*7, 8*). Hence, an alternate model for the surface MoS_2 is that the basal planes are located parallel to the oxide surface (*9*).

Direct experimental evidence for the morphology of the MoS_2 comes from transmission electron microscopy (TEM), which is particularly effective since the interplanar spacing of the basal planes of MoS_2 (hexagonal, space group $P6_3mm$) is large enough (0.613 nm) to be easily resolved. Thus, if a layer of MoS_2 were to lie with its basal plane parallel to the oxide surface, a dark line would be seen at the edge of the oxide support representing a monolayer of MoS_2. A three-dimensional MoS_2 crystallite would appear as an array of dark lines $\approx$0.6 nm apart corresponding to the (002) lattice planes. Indeed, on low-surface-area titania and zirconia supports, isolated dark lines suggestive of MoS_2 bonded to the oxide could be clearly seen (*2*) at the edge of the support when the coverage was below that of a monolayer. At a higher coverage of MoS_2, the dark lines completely covered the oxide surface and multilayers of MoS_2 were also observed. These results would be consistent with the formation of MoS_2 with its basal plane parallel to the oxide surface.

0021-9517/92 $5.00

Similar results were obtained by Delannay (*9*) on low-surface-area $CoAl_2O_4$ samples where the crystals of MoS_2 appear to wrap around the support phase.

On the other hand, on silica and alumina supports, there was no indication of similar dark lines at the edge of the oxide support (*2*). Rather, the dark lines were always located in the interior of the oxide, and it was suggested that the MoS_2 sheets were therefore oriented with their basal planes perpendicular to the oxide support. A similar conclusion was reached by Haydn and Dumesic (*10*) but based on microdiffraction patterns to determine the orientation of the MoS_2 with respect to the planar thin films of alumina which they used as a model support. Previous work by Zaikowski (*11*) on high-surface-area silica came to a similar conclusion, that the MoS_2 sheets were stacked as "bookends" on the silica surface.

Since the morphology of the Mo^{+6} precursor after calcination on TiO_2 and Al_2O_3 is very similar, it is remarkable that after sulfiding, the MoS_2 should adopt such different morphologies. Pratt *et al.* (*2*) suggested that differences in the hydroxyl groups on these supports may contribute to the observed morphology of the sulfide. The IR spectra of hydroxyls on these supports, however, do not reveal significant differences that may account for the altered morphology. There is, however, one significant difference between these supports: notably, their surface areas. Titania is generally available as a low-surface-area powder (for example Degussa P-25 has 65 m^2/g), while γ-alumina and silica used commercially range in surface area from 100–300 m^2/g. The titania powders have larger primary particle sizes (as evident from XRD patterns) and electron micrographs reveal a smoother surface texture compared to the alumina. The markedly different surface textures of the low- and high-surface-area supports may constitute an important factor affecting the morphology of the dispersed MoS_2, which may have been overlooked by previous investigators.

In order to study the role of surface texture and particle size, we have examined the morphology of MoS_2 on low-surface-area model alumina and silica powders and compared it with MoS_2 supported on titania. These model supports allow us to separate the role of surface area and morphology from that of oxide surface chemistry, since all of these supports have comparable surface areas. The objective of this work is to document differences between the morphology of MoS_2 supported on silica, alumina, and titania when powders of comparable surface area are used. The model silica support used for this study contained nonporous spherical particles of silica, 270 nm in diameter, prepared by the method of Stober and Fink (*12*). The Stober spheres were dried in air at 383 K for 2 hr to remove any adsorbed molecular water and their surface area was 15 m^2/g. The model nonporous alumina was prepared by oxidation of aluminum metal using the method of Iijima (*13*) and had a BET surface area of 55 m^2/gm. For comparison, we also used commercial Alon C, which is a fumed alumina prepared by flame pyrolysis of $AlCl_3$ by Degussa Corporation having a surface area of $\sim$100 m^2/gm. The titania used was Degussa titania P-25, which is prepared by the vapor phase pyrolysis of $TiCl_4$ and has a surface area of 65 m^2/gm. We also used a titania-coated silica prepared using the reaction of titanium alkoxide with surface silanols as described elsewhere (*14*).

The samples of titania and titania/silica were physically mixed with MoO_3 and calcined in flowing dry air for 2 hr at 773 K. Previous work shows that this treatment causes the molybdena to spread on the titania forming a monolayer (*15*). The silica and alumina samples were prepared by aqueous impregnation of ammonium heptamolybdate. These were calcined to 573 K in laboratory air. All samples were sulfided at 698 K for 2 hrs in flowing 10% H_2S in H_2. Table 1 summarizes the support surface areas and the analyzed chemical compositions of these materials.

Figure 1 shows a micrograph of the sul-

TABLE 1

Sample Characterization

Support	Surface area (m^2/gm)	Elemental Analysis (wt%) by ICP-AES			
		%Mo	%Al	%Ti	%Si
Alon C	100	2.6 ± 0.1	47.5 ± 0.4	—	—
TiO_2/SiO_2	15	2.7 ± 0.1	—	0.66 ± 0.01	41.5 ± 1.1
TiO_2	65	3.13 ± 0.01	—	54.07 ± 0.07	—
Model alumina	50	20.0 ± 0.01	37.3 ± 0.3	—	—
Model silica	15	2.1 ± 0.01	—		46.0 ± 2.0

fided molybdenum (Mo^{+6}) oxide/TiO_2 sample. This sample was exposed to air during sample preparation for TEM, which involved supporting the powder on 3-mm Cu TEM grids covered by a holey carbon film. Observations were performed in a JEOL JEM-2000 FX electron microscope operated at 200 keV. The presence of MoS_2 on the surface of titania can be clearly seen in the form of dark lines at the edge of the oxide support. These dark lines represent single sheets of MoS_2 lying flat on the surface of

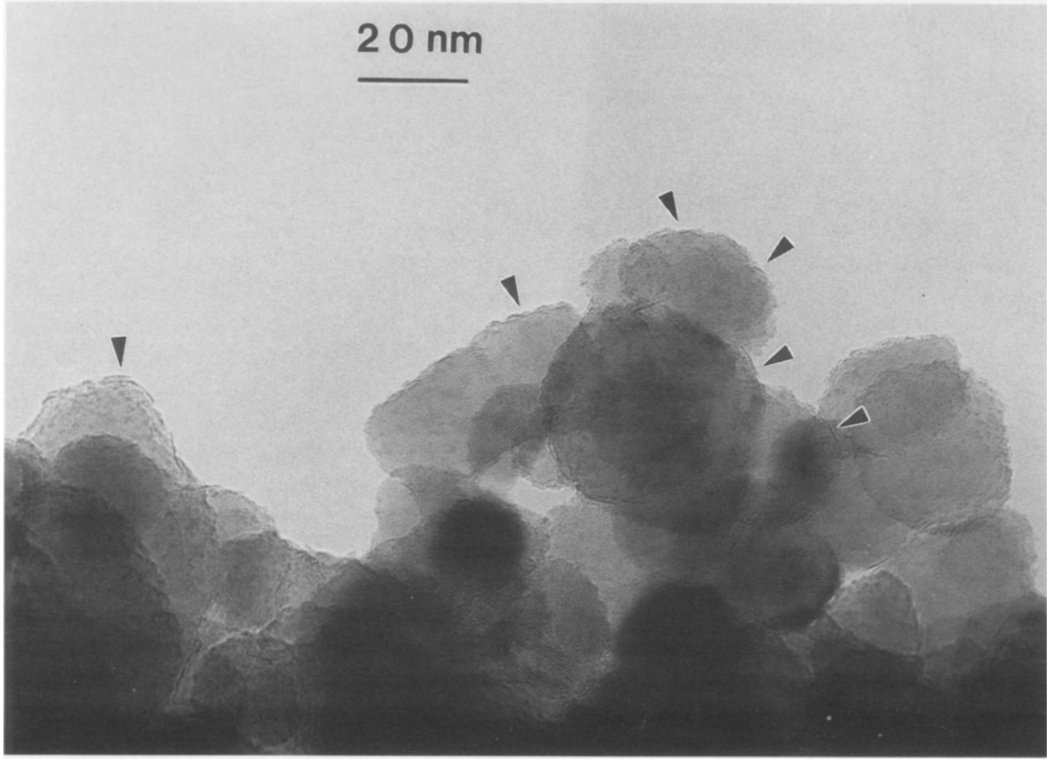

FIG. 1. Micrograph of sulfided molybdenum (Mo^6) oxide supported on Degussa P-25 TiO_2. Small crystals of MoS_2 are seen on the titania surface, as indicated by the arrows.

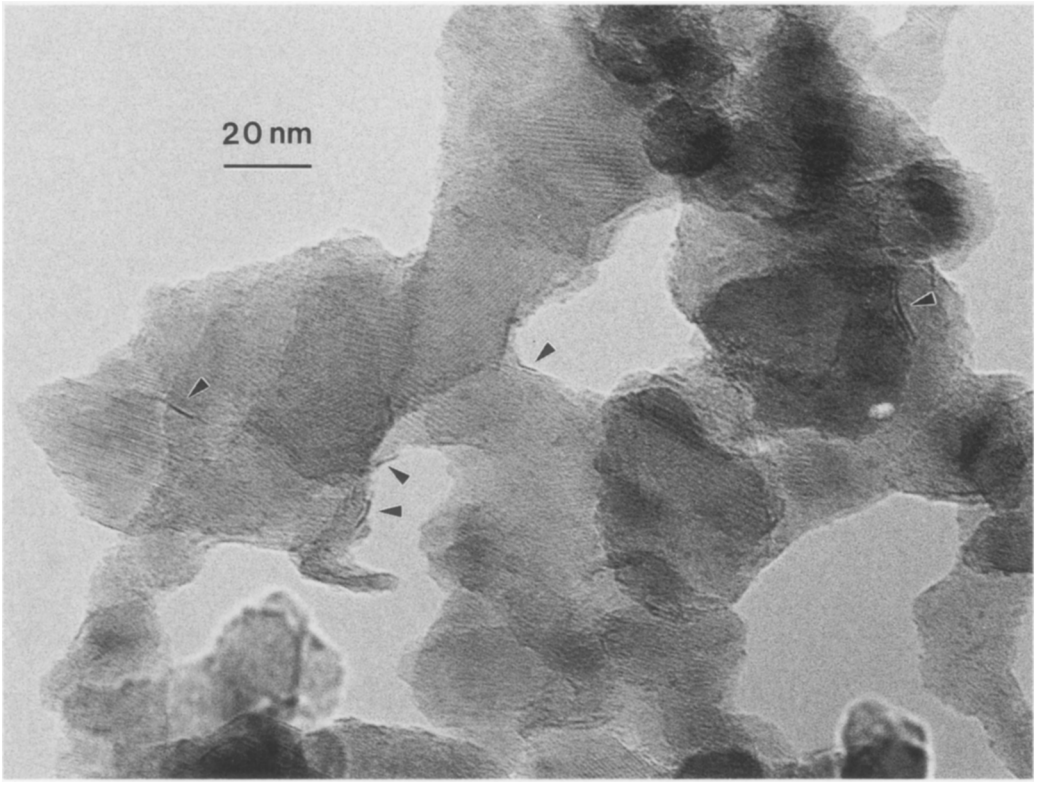

FIG. 2. Micrograph of sulfided molybdenum (Mo^{+6}) oxide supported on Degussa ALON C alumina. Black lines from the basal planes of MoS_2 crystals are visible both on the surface of the alumina and in the interior. The dark lines within the interior appear to be associated with outgrowth on the alumina surface in a direction normal to the image plane.

titania, and the image is similar to that reported by Pratt *et al.* (*2*), who have also confirmed by image calculations that the dark lines corresponds to a single layer of S–Mo–S in the MoS_2 structure. The concentration of Mo in this sample was 3.1 wt%, as determined by ICP-AES, which would be below the monolayer capacity of the titania. This is consistent with the presence only of patches of MoS_2 which do not completely cover the titania surface. Figure 2 shows the sulfided sample of molybdenum (Mo^{+6}) oxide/Alon C, where the majority of the MoS_2 is seen in the interior of the particles, confirming the observations made by Pratt *et al.* (*2*). However, closer examination does reveal a few areas where dark lines can be seen at the edge of the support, indicating that the morphology could be similar to that seen on the titania support.

The morphology of the MoS_2 seen on commercial titania and alumina is now compared with that on several model, nonporous oxide samples having primary particles of controlled morphology. On the sulfided molybdenum (Mo^{+6}) oxide/model alumina (as shown in Fig. 3), where the alumina particles started out as faceted single crystals, sheets as well as stacks of MoS_2 are seen on the alumina surface. The presence of stacks of MoS_2 is consistent with the higher molybdena loading on this sample. Overall, the morphology is very similar to that seen on titania and zirconia in previous work (*2*). The nonporous nature of the model alumina provides unambiguous determination of the

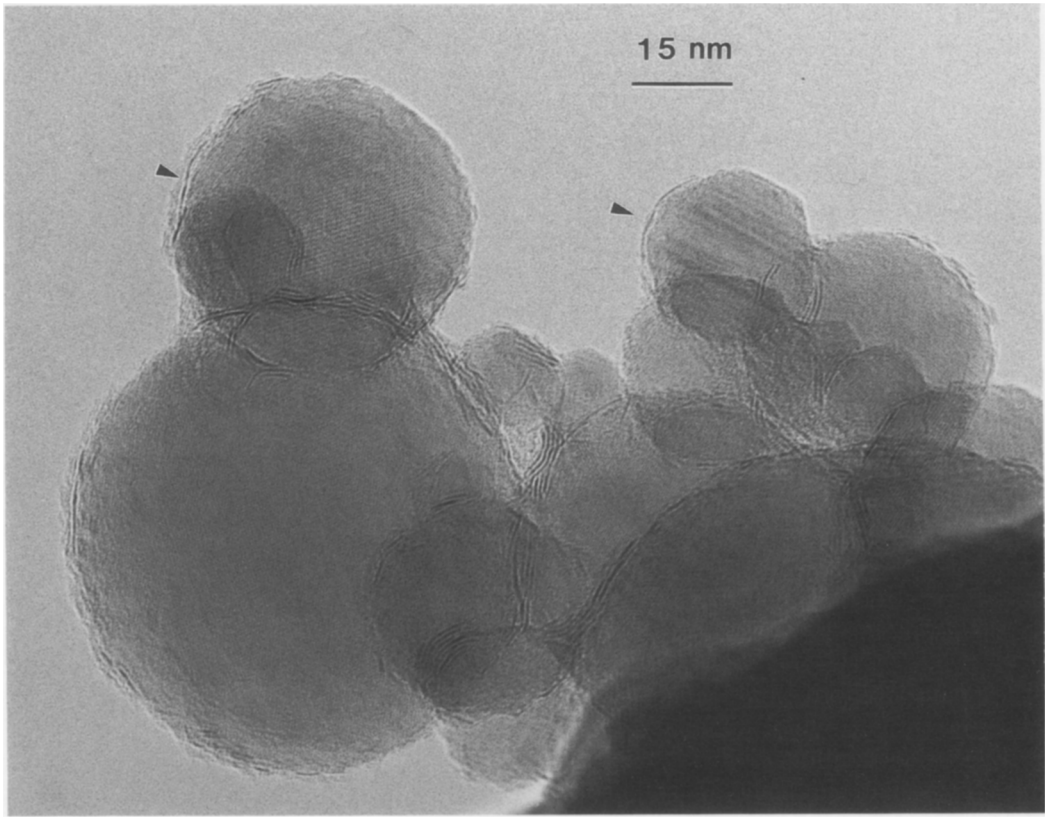

FIG. 3. Sulfided molybdenum (Mo^{+6}) oxide supported on nonporous model alumina. The higher loading of Mo and the low surface area leads to the formation of large MoS_2 crystals imaged as patches of dark lines at the surface of the oxide.

orientation of MoS_2 and shows clearly that the basal plane is parallel to the surface of the oxide. A similar morphology was also seen on the model silica and titania/silica samples shown in Figs. 4 and 5. On silica, small patches of MoS_2 coexist with three-dimensional islands of MoS_2. The high magnification view in Fig. 4a shows that the small patches of MoS_2 indicated by arrows are always located with their basal plane parallel to the oxide support. However, the large three-dimensional island of MoO_3 has transformed into MoS_2 crystallites containing crystal planes randomly oriented with respect to the oxide support. If such a patch of MoS_2 were to be observed in a direction normal to the oxide surface, only the MoS_2 planes normal to the surface would be visible (since the others would not generate any contrast) and hence it would appear as if the MoS_2 sheets were standing up normal to the oxide surface. Figure 4b shows that the MoS_2 multilayers also cause necking of the silica spheres. Figure 4c shows a higher magnification view of this sample, showing clearly a few small segments of dark lines representing MoS_2 monolayers on the nonporous silica.

Micrographs from the titania–silica sample, before and after sulfiding, are shown in Fig. 5. This sample contained titania in excess of the monolayer capacity of this silica and the excess titania could be imaged as small bumps arrowed in Fig. 5a. The molybdena layer on the surface of the titania/silica cannot be directly imaged due to inad-

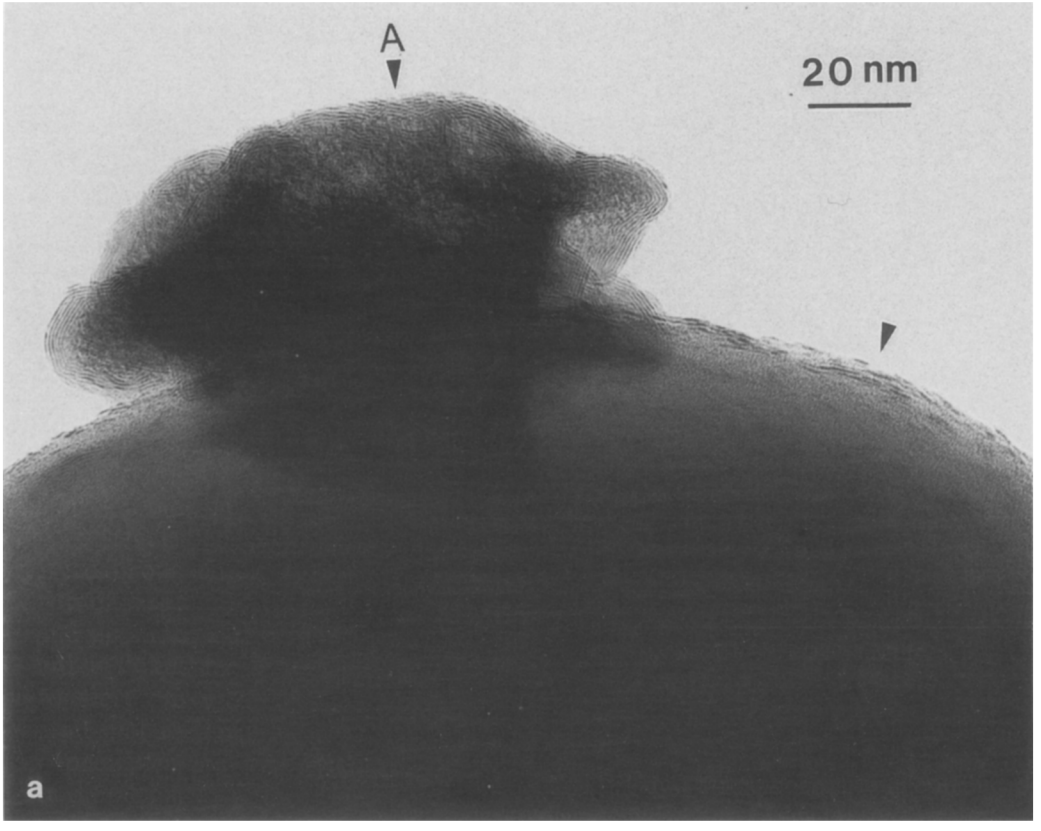

FIG. 4. Sulfided molybdenum (Mo^{+6}) oxide supported on nonporous model silica. (a) High-magnification view showing small segments of dark lines corresponding to MoS_2 crystals (arrowed) and a large crystal of MoO_3 (marked A) which has also transformed into MoS_2. (b) Low-magnification view showing the necking of the silica spheres caused by the presence of MoS_2. (c) A high magnification view showing single segments of dark lines representing MoS_2 monolayers on the nonporous silica.

equate contrast. However, after sulfiding, the dispersed molybdenum (Mo^{+6}) oxide phase on the surface of the titania is transformed to MoS_2 giving rise to the characteristic single or multiple dark lines arrowed in Fig. 5b. A large particle of TiO_2 is also seen in this micrograph (marked "A") whose surface is covered by small segments of dark lines. Some dark lines also appear within the interior of this titania particle and could be interpreted as MoS_2 located with its basal plane normal to the oxide support. However, the three-dimensional nature of this titania particle makes it equally likely that the dark lines come from a crystalline particle of MoS_2 located on top of a grain of titania.

The results of this study show clearly that the MoS_2 in the sulfided and air-exposed sample always occurs with its basal planes parallel to the oxide surface. We have found no evidence for MoS_2 bookends where the basal planes are stacked up perpendicular to the oxide surface on any of the supports used in this study. Thus, in contrast to observations reported previously (*2*), we find no difference between the behavior of TiO_2, SiO_2 and Al_2O_3 when used as a support for MoS_2. The bookend morphology of MoS_2 deduced by previous workers (*2*) was based

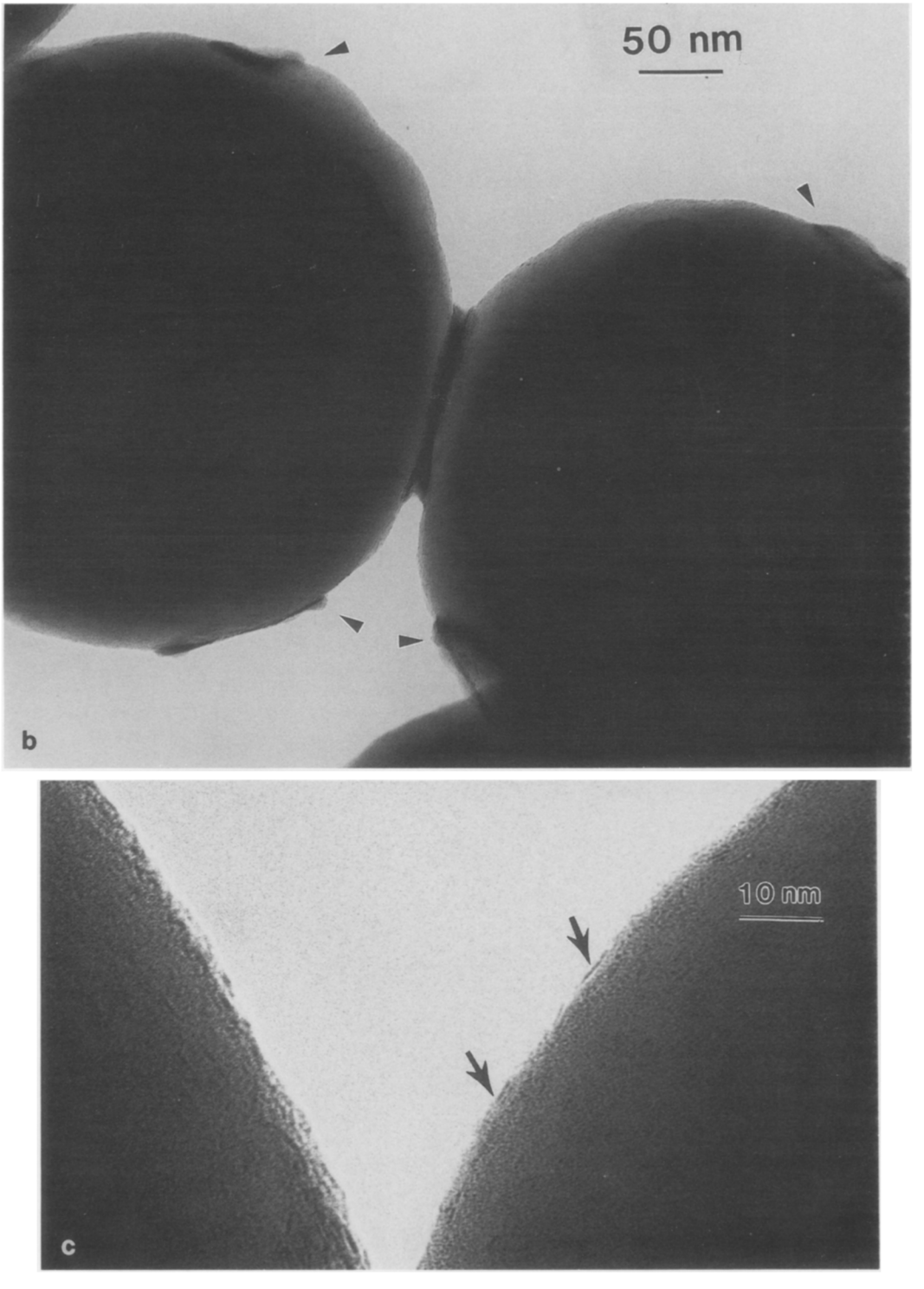

FIG. 4—*Continued*

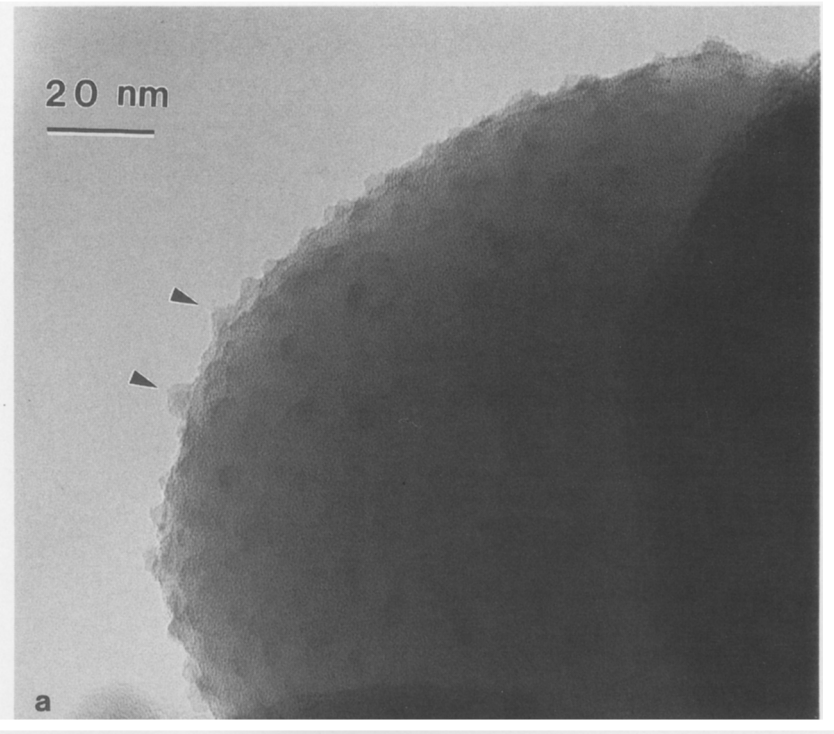
20 nm
a

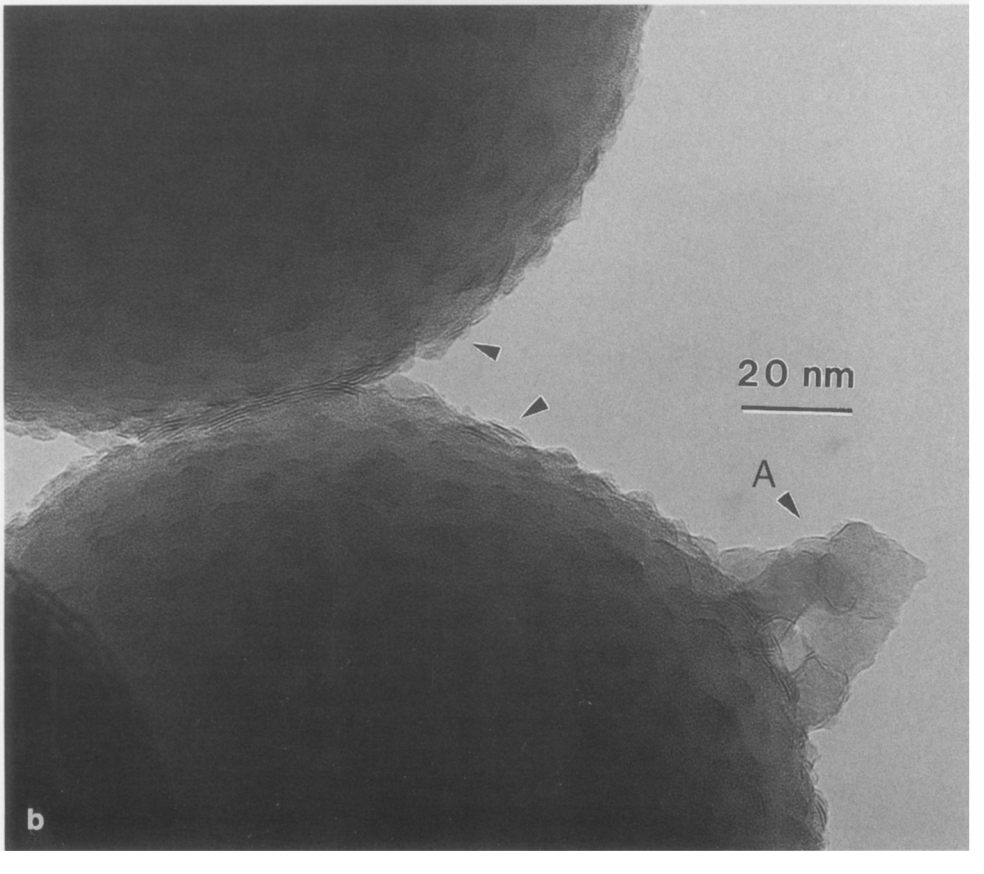
20 nm
A
b

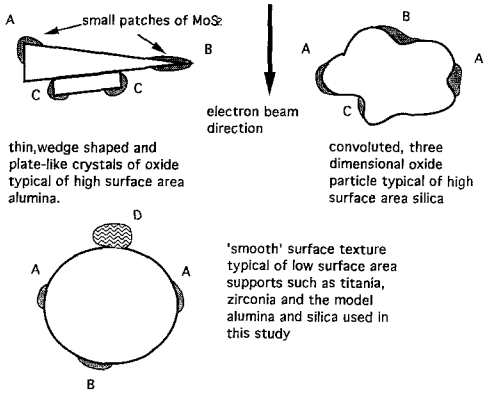

A - MoS2 monolayer that would be imaged as a dark line at the edge of the oxide support when viewed in projection
B - MoS2 monolayer that would not be imaged in projection since the basal planes are not suitably oriented for diffraction
C - MoS2 monolayer that would be imaged as if the basal planes were perpendicular to the support when viewed in projection
D - Crystallite of MoS2 with randomly oriented (002) planes of MoS2, where only the planes normal to the support would show up as dark lines when imaged in projection.

FIG. 6. Schematic diagram showing how surface texture could affect the visibility of MoS_2 on oxide surfaces.

on the absence of a dark line at the edge of the support particles. It is important to recognize that the electron micrograph represents a projection of the three-dimensional sample along the beam direction. Thus, dark lines originating from the MoS_2 would typically be seen only when an MoS_2 sheet of sufficient size is oriented along the beam direction. If the primary oxide particles occur as thin plate-like or wedge-shaped crystals that lie flat on the carbon supporting film on the TEM grid, any MoS_2 at the edge would not be readily imaged. This possibility is depicted as the particle "B" in Fig. 6. MoS_2 monolayers that have a sufficient depth along the beam direction would appear as dark lines either at the edge of the oxide (as in "A") or within the bulk of the oxide (shown as "C"). However, dark lines seen within the oxide support may well arise from a part of the oxide surface that is located parallel to the beam direction, i.e., a surface step. We suspect that MoS_2 crystals shown as "C" in Fig. 6 may have been identified in previous work as bookends. The probability of observing MoS_2 layers with their basal plane parallel to the surface of the support would be enhanced considerably with nonporous oxide particle, and it is precisely from such low surface area supports that the basal plane-bonded morphology of MoS_2 has been deduced. Figure 6 also shows three-dimensional particles of sulfided molybdenum (Mo^{+6}) oxide (marked "D") where the sheets of MoS_2 are randomly oriented but would yield images suggestive of the bookend morphology, when observed in projection.

In conclusion, we feel that the observed bookend morphology on high-surface-area supports is an artifact of the electron microscopic examination of these materials, since the images always represent a projected view of a three-dimensional sample. It is evident that the surface texture of the support could play a major role in determining the morphology of the MoS_2. A support such as alumina that has a microscopically rough surface texture would tend to favor formation of numerous small crystals of MoS_2, while a low-surface-area support such as titania having a "smooth" surface and fewer nucleation sites would favor formation of fewer MoS_2 islands of larger size. Thus, on titania one would expect increasing Mo loading to lead to an increase in the size of MoS_2 islands and a corresponding lowering

FIG. 5. Molybdenum (Mo^{+6}) oxide supported on titania/silica (a) before and (b) after sulfiding in 10% H_2S/H_2 at 700 K. The bumps arrowed in (a) are small three-dimensional islands of titania that are coated with molybdenum (Mo^{+6}) oxide. After sulfiding, the presence of surface MoS_2 is seen in (b) as characteristic dark lines on the titania bumps (arrowed). A large particle of titania (marked A) is also covered by dark lines on the surface corresponding to the presence of MoS_2. Some of the dark lines are also seen within the interior of this particle.

of the number of edge/basal plane sites. The data of Pratt *et al.* (2) does indeed show a marked fall-off in specific activity for thiophene HDS on Mo/titania with increasing Mo loading, but no similar drop on Mo/alumina. These results suggest that the surface texture of the oxide support may be an important factor affecting the morphology, and indirectly the reactivity, of the dispersed phase in a heterogeneous catalyst.

ACKNOWLEDGMENTS

Financial support via NSF Grant CTS 89-12366 is gratefully acknowledged. The portion of the work performed at Sandia National Laboratories was funded by the U.S. Department of Energy, Office of Fossil Energy, Advanced Research and Technology Development Program. We thank E. P. Boespflug for experimental assistance in sulfiding of these samples. Transmission electron microscopy was performed at the Microbeam Analysis Facility in the UNM Department of Geology.

REFERENCES

1. Gates, B. C., Katzer, J. R., and Schuit, G. C. A., "Chemistry of Catalytic Processes." McGraw–Hill, New York, 1979.
2. Pratt, K. C., Sanders, J. V., and Christov, V., *J. Catal.* **124,** 416 (1990).
3. Massoth, F. E., *Adv. Catal.* **27,** 265 (1978).
4. Chung, K. S., and Massoth, F. E., *J. Catal.* **64,** 320 (1980).
5. Hall, W. K., *in* "Chemistry and Physics of Solid Surfaces VI" (R. Vanselow and R. Howe, Eds.), p. 73. Springer-Verlag, Berlin/New York, 1986.
6. Zmierczak, W., Qader, Q., and Massoth, F. E., *J. Catal.* **106,** 65 (1987).
7. Clausen, B. S., Topsoe, H., Candia, R., Villadsen, J., Lengeler, B., Als-Nielsen, J., and Christensen, F., *J. Phys. Chem.* **85,** 3868 (1981).
8. Huntley, D. R., Parham, T. G., Merrill, R. P., and Sienko, M. J., *Inorg. Chem.* **22,** 4144 (1983).
9. Delannay, F., *Appl. Catal.* **16,** 135 (1985).
10. Haydn, T. F., and Dumesic, J. A., *J. Catal.* **103,** 366 (1987).
11. Zaikowski, V., Plynsova, L. M., Burmistrov, V. A., Startsev, A. N., and Yermakov, Yu, I., *Appl. Catal.* **11,** 15 (1984).
12. Stober, W., Fink, A., and Bohn, E., *J. Colloid Interface Sci.* **26,** 62 (1968).
13. Iijima, S., *Jpn. J. Appl. Phys.* **23,** L347 (1984).
14. Srinivasan, S., Datye, A. K., Smith, M. H., Wachs, I. E., Deo, G., Jehng, J. M., and Turek, A. M., *J. Catal.* **131,** 260 (1991)
15. Stamfl, S. R., Chen, Yi, Dumesic, J. A., Niu, C., and Hill, C. G., *J. Catal.* **105,** 445 (1987).

S. Srinivasan
A. K. Datye

Department of Chemical & Nuclear Engineering
University of New Mexico
Albuquerque, New Mexico 87131

C. H. F. Peden

Sandia National Laboratories
Albuquerque, New Mexico 87185

Received November 13, 1991; revised April 7, 1992